2023-02-14

Changes in the mechanical performance of an ortho-planar spring after aging tests

Lucas F. L. Santos
Pontifical Catholic University of Rio de Janeiro (PUC-Rio), lucasferreiralimasantos@gmail.com

Larry L. Howell
Brigham Young University - Provo, lhowell@byu.edu

Jose J. R. d'Almeida
Pontifical Catholic University of Rio de Janeiro (PUC-Rio)

Original Publication Citation

Santos, L.F.L., d'Almeida, J.R.M., Howell, L.L., "Changes in the mechanical performance of an ortho-planar spring after aging tests," Journal of the Brazilian Society of Mechanical Sciences and Engineering, Vol. 45, No 2, article 118, https://doi.org/10.1007/s40430-023-04049-5, 2023.

Changes in the mechanical performance of an ortho-planar spring after aging tests

Lucas F. L. Santos, José R. M. d'Almeida and Larry L. Howell*

L. F. L. Santos, Prof. J. R. M. d'Almeida
Department of Chemical and Materials Engineering (DEQM), Pontifical Catholic University of Rio de Janeiro (PUC-Rio), Rua Marquês de São Vicente, 225 – Gávea, Rio de Janeiro, RJ 22430-060, Brazil
E-mail: lucasferreiralimasantos@gmail.com

Prof. L. L. Howell
Department of Mechanical Engineering, Brigham Young University, Provo, Utah 84602, United States of America

Keywords: ortho-planar spring, compliant mechanism, aging tests, mechanical performance

This paper analyzed an ortho-planar spring (OPS) compliant mechanism and evaluated its mechanical performance after hygrothermal and ultraviolet radiation aging tests. The aging analysis performed here addresses the performance of compliant mechanisms after aging processes which can help inform the design of future compliant mechanisms. ASTM D638 tensile test type I samples were also submitted to aging to serve as a comparison for OPS samples. The samples were submitted to three different kinds of aging conditions, namely water immersion, oil immersion, and ultraviolet radiation. In conclusion, tensile samples showed significant statistical changes in Young's modulus and elongation at break, whereas OPS samples did not show significant statistical changes in any aging condition, indicating that aging processes at the time interval analyzed in this work did not affect the mechanical properties and elastic capabilities of the samples. Although tests using the specific materials, environment, and exposure time would be needed to verify the use in a specific application, the results of this study suggest that compliant mechanisms show promise for implementation in applications where aging is a concern and their life is expected to be within the bounds of this aging study.

1. Introduction

Compliant mechanisms (CM) use the deflection of their flexible members to generate motion, and some of their advantages include simple manufacturing, no need for lubrication, and less stocking of components[1]. On the other hand, rigid mechanisms rely on movable joints to have mobility and present the need for lubrication and a time-consuming assembly.

Works related to the development of new design of CMs can be easily found, with applications in areas like medicine, automotive and robotics [2-7].

One of the main motivations for this work is to address the need to better understand the aging effects of compliant mechanisms. Despite their widespread use in various applications, there has been a lack of research on the long-term effects of environmental factors such as UV exposure, water immersion, and oil immersion on CMs. It is helpful to select common compliant mechanism configuration as a general surrogate for compliant mechanisms such that the device has a structure and performance common to many compliant mechanisms. Therefore, in this study, an ortho-planar spring developed by Parise et al. [8] was selected as the CM for testing due to its widespread use in previous studies [20-22] and its general usefulness as a compliant mechanism. The results of this study provide valuable data on the aging behavior of CMs and highlight the importance of understanding the long-term effects of environmental factors on these mechanisms. This information is crucial for ensuring the reliability and durability of CMs in practical applications.

Figure 3 shows the OPS geometry that will be used throughout this work. It was selected because it has well-defined geometry, is capable of large deflections, and has behaviors common in compliant mechanisms so can act as a surrogate for compliant mechanisms in this aging study. While the configuration shown in Figure 3 was designed to be part of a pneumatic valve positioner [8], it has a wide range of applications. For example, it was used to replace a large coil spring in a continuously variable transmission common in off-road vehicles [Rasmussen et al., Whiting et al.] Many other applications have been demonstrated, including robotics [Qi et al.], energy harvesting [Dhote et al.], precision sensors [Shi et al., Ataollahi et al.], check valves for microfluidic devices [Nguyen et al.], tactile arrays [Konstantinova et al.], microneedle arrays [Teichert et al.], micropositioning [Lyu and Xu], to name a few.

A mechanism leg is the union of an intermediate platform and its associated flexible members. This mechanism consists of three legs, six flexible members, and three intermediate platforms.

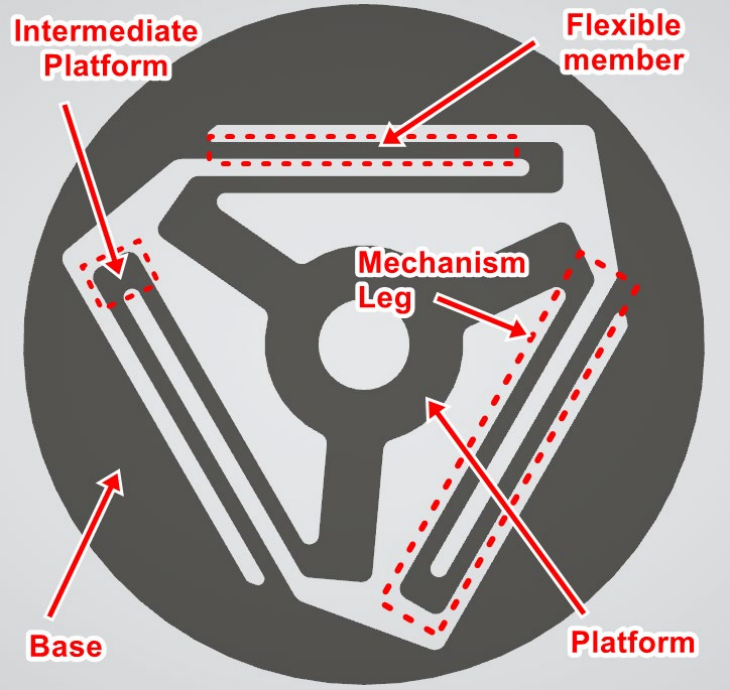

Figure 3. Geometry terms of the ortho-planar spring specimen.

Parise et al. [8] demonstrated a potential application for this mechanism. An ortho-planar spring made with stainless steel was utilized to control the flow of air in an industrial pneumatic valve for an international valve manufacturer.

However, as many CMs are fabricated from polymeric materials, they can suffer from the effect of environmental agents. It is well known that polymers present considerable chemical, physical or mechanical changes after an aging period [9-14]. Therefore, it becomes essential that the applications of CMs consider the possible aging effects of the environment.

The most common aging conditions are exposure to UV and water. Water aging is performed by simulating humid environments or by accelerated testing by fully immersing the samples in a water bath. However, depending on the application, such as in oil and gas industries, the material can be exposed to oil. Exposure to UV radiation affects the surface of the polymer

and may cause chemical and color changes [13]. Works also report the appearance of microcracks in polymers and polymer matrix of composites and the scission of polymer chains a consequence of UV exposure [15,16].

When analyzing the effect of liquid and temperature, polymers usually present different behaviors depending on the temperature it is submitted to. Normally, the degradation is accelerated with the increase of temperature [17], but if the aging temperature is not close to the glass-transition temperature (T_g) of the polymer, the saturation levels of absorption do not change with temperature. When these temperatures are close to T_g, chemical changes are induced in the material, which allows higher levels of moisture content [18,19].

2. Materials and Methods

Two types of specimens were analyzed in this work. The first one is an ASTM D638 tensile test type I specimen (**Figure 4**) and the other is an ortho-planar spring compliant mechanism (**Figure 5**), where the flexible members had 3.6mm of thickness and a length of 51.5mm [23]. Both were 3D printed with acrylonitrile butadiene styrene (ABS) in a GTMax3D H5 printer with the printing parameters listed in **Table 1**.

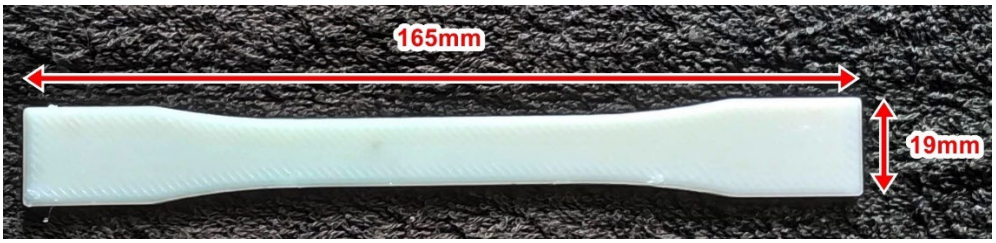

Figure 4. ASTM D638 tensile test type I specimen.

Figure 5. Ortho-planar spring compliant mechanism.

Table 1. 3D printing settings used for the fabrication of tensile and OPS samples.

Printing Settings	Values
Material	ABS
Layer height (mm)	0.3
Infill percentage	100%
Temperature (°C)	220 (nozzle) and 110 (heated bed)
Printing speed (mm/s)	60
Raster angle	45°/-45°

Although the infill percentage parameter was set to be 100%, the samples presented significantly lower values. To calculate an approximation of the infill, the weight, thickness, and surface area of the specimens were used. The global average value for tensile samples

was 74.6% and 91.3% for OPS samples. This infill difference will be discussed further in the results and discussions section.

The specimens were submitted to seven aging conditions, namely, UV exposure, water immersion (room temperature, 50°C, and 70°C), and oil immersion (room temperature, 50°C, and 70°C). The choice of these aging conditions is because since many potential CM applications would require them to spend some of their life exposed to UV or water. As many rigid mechanisms have contact with oil, it is fair to think that in the future, CMs can replace or assist those rigid mechanisms, which becomes important that the oil immersion aging analysis is considered.

The room temperature (RT) aging samples were placed in a closed drawer to avoid significant temperature changes and UV exposure. The room temperature was approximately 23 ± 0.5°C. All liquid immersion aging samples were put inside a glass recipient and placed in laboratory water bath equipment. The UV specimens were placed in a dark chamber with LED light of 254 nm and power of 8 W. All aged specimens underwent aging for 4,320 hours (6 months). For the aging and as received (AR) conditions, three samples of each specimen type were used.

2.2. Mechanical Testing

Both specimens were mechanically tested in an AME-2kN universal testing machine. Tensile samples were placed on tensile grips, with a distance of 115 mm between them. Tensile tests were conducted at a rate of 5 mm/min.

As shown in **Figure 5**, to test OPS samples, a different setup was necessary. An auxiliary black ABS part was 3D printed and attached to serve as the sample base. The samples' centers were connected to the moving jaw of the equipment. The samples were then bolted and screwed to the base to minimize lifting during the tests. The samples were pulled up at a rate

of 5 mm/min. This vertical movement setup was chosen to simulate real-life applications of industrial valves as shown in the work of Parise et al. [8].

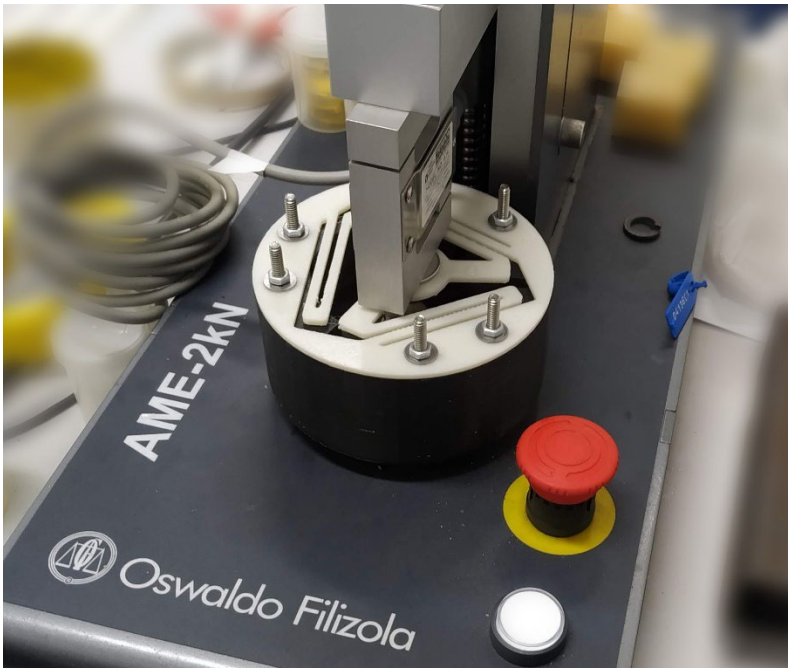

Figure 5. Mechanical setup of OPS samples.

The tensile samples were loaded until rupture, whereas the OPS samples were loaded to a maximum displacement of 20% of the flexible member length (FML), or 10.30 mm.

2.3. Colorimetric tests

To properly analyze the color change of samples before and after aging, colorimetric tests were performed on both specimens using the Delta Vista 450g (**Figure 6**) equipment from the company Delta Color. A total of ten measurements were taken on each sample to reduce test error.

Figure 6. Colorimetry equipment Delta Vista (Delta Color).

The settings used in the measurements were: D65 illuminant, observer 10°, optical geometry 45/0° with a brightness of 60° e circular measurement area of 4 mm of diameter.

The CIE L*a*b* color scale was the chosen system for the results and can be represented by a Cartesian coordinate system. The L* is the one that defines the luminosity between light (negative L*) and dark (positive L*), a* is the one associated with the variation of the red color (positive a*) and green (negative a*), and b* is the one associated with the variation of the yellow (positive b*) and blue (negative b*) [24].

To compare the color of samples from an aging condition to AR samples, the expression of **Equation 1** was used, where E stands for difference in color of samples and ΔL*, Δa* and Δb* stand for differences in luminosity, red/green axis difference, and yellow/blue axis difference, respectively.

$$\Delta E = \sqrt{(\Delta L^*)^2 + (\Delta a^*)^2 + (\Delta b^*)^2} \quad (1)$$

The perception of color change varies from one person to another. To distinguish color variations, color intervals of E were created as follows [13]:

- $\Delta E < 1$: color change is not noticed by human eyes.
- $1 \leq \Delta E < 3.3$: color change is noticed by trained operators only.
- $\Delta E \geq 3.3$: color change is noticed by anyone.

These intervals were used to analyze color changes in tensile and OPS samples. When compared to AR samples, the variations of L*, a*, and b* were also analyzed to check if samples were lighter/darker (L*), redder/greener (a*), and yellower/bluer (b*).

3. Results and Discussions

To facilitate the analysis of the results, the specimens are represented by symbols as follows: as received (AR), ultraviolet radiation (UV), water immersion at room temperature (WI-RT), water immersion at 50°C (WI-50), water immersion at 70°C (WI-70), oil immersion at room temperature (OI-RT), oil immersion at 50°C (OI-50) and oil immersion at 70°C (OI-70). Unless otherwise stated, the variations will be relative to the AR samples.

The varying infill percentages of samples affect the comparison of aged and AR samples. To overcome this, linear interpolation can be used to correct mechanical properties based on infill differences, as properties tend to increase linearly after 70% infill [25]. If the samples of a certain condition, for example, have an infill higher than AR samples, then the original properties of these samples would be higher. For any aging condition and property, the correction procedure consisted of calculating an approximation of the samples' original properties before aging and using this value as a base to check the true variation of these properties, as shown in **Figure 7**. Ideally, the materials used for each sample would be similar, i.e., the same infill percentage should be the same. Because that is not the case here, the value of the original properties of the samples will be assumed to be equal to the properties of AR samples, and the variation calculated considering the calculated properties will be applied. In Figure 5, as an example, the Young's modulus property of the samples was considered to be 500MPa and the variation of -23.8% was applied, creating a corrected property value that can be safely used in the statistical tests. It is important to say that this correction procedure assumes that samples with different infills will present equal variations

in properties when submitted to an aging condition. Thus, this procedure aims to approximate the true variations, given that infill percentages can influence how aging affects the samples.

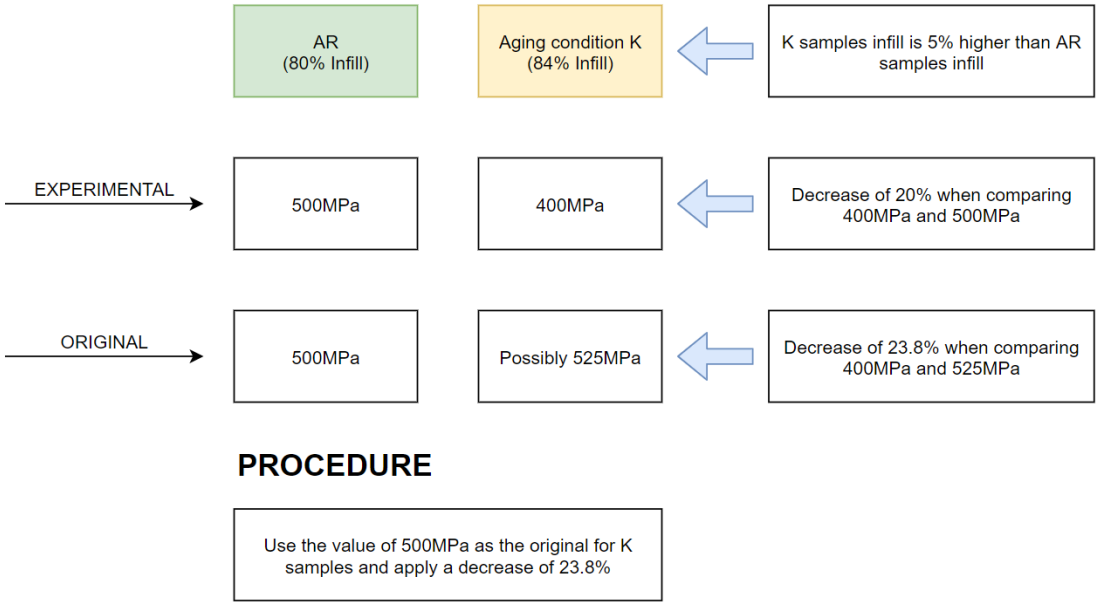

Figure 7. Ortho-planar spring compliant mechanism.

Student's t-tests were used on both types of specimens to check if the variations in mechanical properties were due to aging and if the means were statistically different from one another. The mean values of the properties were compared between an aging condition and AR samples. For this statistical analysis, the t-test with equal sample sizes was chosen. The null hypothesis states that two samples' means are statistically equal. As the sample size (n=3) is small, a level of significance of 10% was chosen, implying that the null hypothesis is accepted if the p-value is smaller than or equal to 0.9. If the value is greater than 0.9, the alternative hypothesis is accepted, indicating that the means are statistically different.

3.1. Tensile samples

Mechanical tensile tests were performed on the tensile test type I specimen. The mechanical properties of the samples of each condition, such as Young's modulus, ultimate strength, elongation at break, and toughness, are listed in **Table 2**. **Figure 8** shows the plot of one tensile sample from each condition. Because all of the samples' failures were brittle, only the

toughness was calculated, since it would be impossible to distinguish the elastic and plastic zones. The plots of the tensile tests of all samples can be found in the Supporting Information in **Figure S1**, **S2**, **S3**, **S4**, **S5**, **S6**, **S7** and **S8**.

Table 2. Mechanical properties of the tensile test type I samples.

Condition	Young's modulus [MPa]	Ultimate strength [MPa]	Elongation at break [%]	Toughness [MJ/m³]
AR	640.4 ± 83.4	17.5 ± 2.2	4.1 ± 0.1	0.41 ± 0.07
UV	574.9 ± 24.7	17.6 ± 2.2	3.4 ± 0.2	0.33 ± 0.06
WI-RT	636.7 ± 110.2	19.1 ± 3.8	4.0 ± 0.6	0.41 ± 0.09
WI-50	550.9 ± 79.9	16.9 ± 5.1	4.1 ± 0.4	0.40 ± 0.15
WI-70	520.6 ± 50.5	16.5 ± 4.3	3.7 ± 0.5	0.34 ± 0.13
OI-RT	537.9 ± 63.8	16.2 ± 3.6	4.2 ± 0.5	0.41 ± 0.13
OI-50	518.7 ± 41.5	16.7 ± 3.5	4.4 ± 0.4	0.45 ± 0.10
OI-70	574.8 ± 5.4	19.5 ± 0.3	4.8 ± 0.2	0.56 ± 0.04

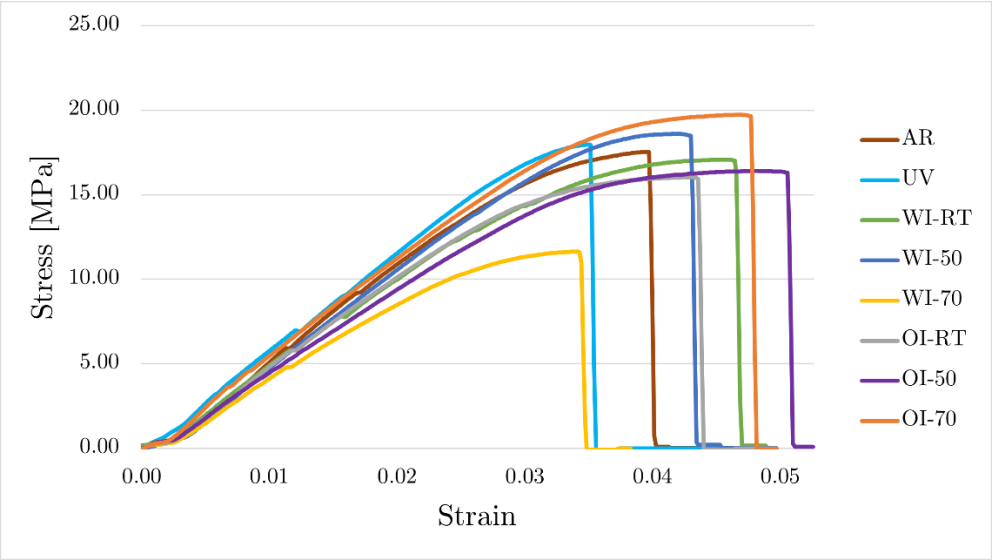

Figure 8. Tensile tests of one tensile sample of each condition.

The mechanical properties of tensile samples were corrected, and the p-value for each condition of the Student's t-test for all properties is listed in **Table 3**. The variations using the corrected mechanical properties are shown in **Figure 9**. Unless otherwise stated, discussions of results are based on the corrected values.

Table 3. The p-value of the Student's t-test of the corrected mechanical properties of the tensile samples.

Condition	Young's modulus	Ultimate strength	Elongation at break	Toughness
AR	-	-	-	-
UV	0.9315	0.6335	0.9982	0.9291
WI-RT	0.6117	0.6475	0.7124	0.5512
WI-50	0.8553	0.5384	0.5828	0.5167
WI-70	0.9438	0.6087	0.7519	0.7319
OI-RT	0.9186	0.6872	0.6695	0.5128
OI-50	0.6943	0.6056	0.9078	0.7124
OI-70	0.9478	0.7325	0.9835	0.9740

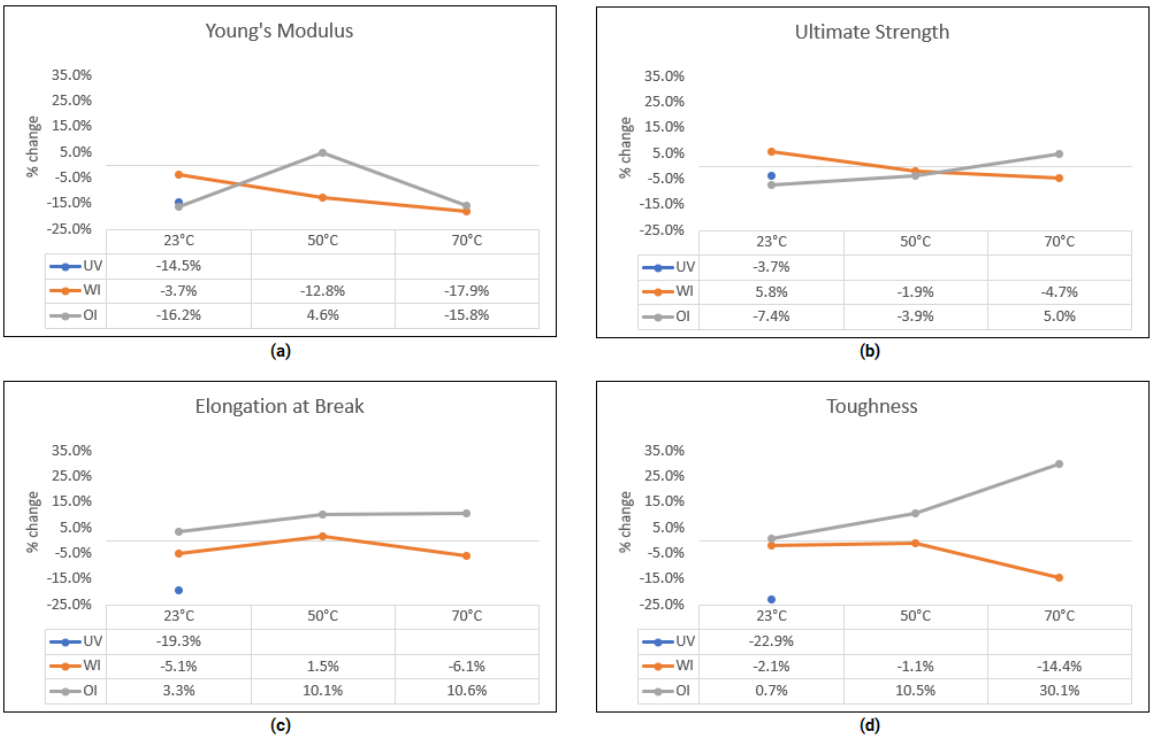

Figure 9. Variations of the mechanical properties of the tensile samples as a function of temperature.

It is worth noticing that the tensile testing of two WI-RT samples was terminated before they could break due to a problem with the test equipment. As a result, the variation in ultimate strength could be greater than +5.8%. As a result, the ultimate strength will be determined by the maximum achieved stress value.

Specimens submitted to hygrothermal aging were already expected to present inferior mechanical properties. In WI samples, the decrease in Young's modulus was only significant at 70°C with a variation of -17.9%, because higher temperatures can cause faster plasticization, more aggressive hydrolysis, or swelling-induced microcracking [26]. In fact, this was the only significant statistical variation in WI samples, despite the fact that the results show a downward trend in properties. All WI samples presented non-significant decreases in toughness, i.e., the values were statistically equal to AR samples.

Amaral investigated the deterioration of properties in oil-aged polymers [24]. The Young's modulus decreased in both samples in the study (PA 12 and HDPE). HDPE samples showed an increase in ultimate strength, whereas PA 12 samples showed a decrease.

Young's modulus values for OI samples were statistically lower at room temperature and at 70°C in this study. The Young's modulus and Ultimate Strength of the OI-50 samples were found to be statistically equal to the AR samples' properties, implying that the aging had no effect on the mechanical properties of these samples.

In OI samples, the elongation at break increased, particularly in OI-70 samples, where it increased 10.6%. The toughness followed the same pattern and increased. This increase could be the result of enhanced material flexibility, as Pereira et al. [27] observed in oil aged HDPE. OI-RT and OI-50 samples were statistically equal in toughness and elongation at break when compared to AR samples.

The samples' weights were measured before and after the aging processes, and the results are listed in **Table 4**. UV samples had a greater weight variation than WI samples, and a significant amount of liquid was absorbed in all hygrothermal conditions. OI samples had higher variations than WI samples, indicating that ABS absorbs more oil than water. The infill percentage values of the tensile samples shown in Section 2 can explain these large variations. The lower the infill, the more voids there are inside the structure, which implies more paths for liquid to enter and interact.

Table 4. Weight of the tensile samples before and after the aging processes.

Condition	Weight [g]	Weight after [g]	Variation
AR	6.4 ± 0.6	-	-
UV	6.7 ± 0.5	7.7 ± 0.5	+20.1%
WI-RT	6.6 ± 0.6	7.2 ± 0.4	+12.4%

WI-50	6.3 ± 0.9	7.5 ± 0.7	+16.0%
WI-70	6.3 ± 0.7	7.4 ± 0.7	+15.4%
OI-RT	6.4 ± 0.7	7.6 ± 0.4	+18.7%
OI-50	6.5 ± 0.6	7.8 ± 0.4	+20.6%
OI-70	6.8 ± 0.1	8.1 ± 0.1	+25.4%

Studies often report an increase of the Young's modulus after UV exposure [12,28]. Here, UV samples showed a 14.5% decrease. This could be due to the significant amount of moisture absorbed inside the UV dark chamber, which causes plasticization and, as a result, a decrease in molecular interactions [29]. Moisture absorption would be much lower if samples had a higher infill, and the true impact of UV could be better analyzed.

Kakanuru and Pochiraju [30] reported a maximum moisture gain of only 0.67% in their 3D printed ABS samples with 100% infill submitted to distilled water at 50°C. Therefore, the weight variations were indeed associated with the infill percentage.

When compared to other works in the literature, **Table 5**, the Young's modulus and ultimate strength of this work's AR samples are significantly lower, which can be attributed to the use of a different fabrication process or 3D printers. The tensile samples were also less stiff than expected due to the reduced infill percentage.

Table 5. Comparison of the mechanical properties of AR tensile test type I samples to works in the literature.

Reference (Fabrication Process)	Young's Modulus [MPa]	Ultimate Strength [MPa]	Elongation at Break [%]
This work (3D printed)	640.40 ± 83.41	17.46 ± 2.21	4.04 ± 0.12

Fiorio et al. [28] (injection molded)	1950 ± 70	32.2 ± 0.2	-
Kakanuru and Pochiraju [30] (3D printed)	2800	38.64	3.41
Popescu et al. [31] (3D printed)	1833.33	21.66	1.50

The most noticeable color change was seen in UV, WI-70, and OI-70 samples. OI-70 samples were lighter than WI-70 samples despite oil absorption, indicating possible chemical degradation of WI-70 samples. The color of WI-70 and OI-70 samples shifted from white to a brown scale, while UV samples tended to a light-yellow tone. **Figure 10** shows the samples from all of the conditions.

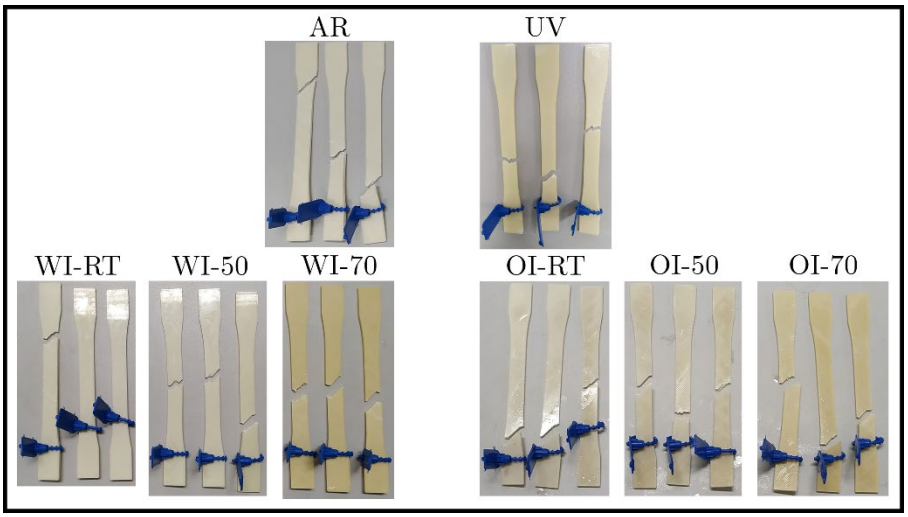

Figure 10. Tensile samples after aging and mechanical tests.

Colorimetric tests were performed on tensile samples, and the values of ΔE, ΔL*, Δa*, and Δb* for each condition are listed in **Table 6**.

Table 6. Values of ΔE, ΔL*, Δa*, and Δb* of the tensile samples.

Condition	ΔE	ΔL*	Δa*	Δb*
AR	-	-	-	-
UV	11.2 ± 0.9	-1.6 ± 1.0	-0.4 ± 0.2	11.0 ± 0.9
WI-RT	1.7 ± 1.2	-0.1 ± 2.0	0.2 ± 0.3	-0.6 ± 1.2
WI-50	1.4 ± 0.8	1.1 ± 1.2	-0.2 ± 0.1	0.0 ± 0.8
WI-70	9.4 ± 0.8	4.1 ± 1.5	2.3 ± 0.2	8.0 ± 0.7
OI-RT	2.5 ± 0.3	-1.8 ± 0.7	0.2 ± 0.1	-1.6 ± 0.4
OI-50	4.2 ± 2.0	-4.1 ± 2.1	0.2 ± 0.1	-0.8 ± 0.7
OI-70	8.4 ± 1.4	-6.1 ± 2.5	0.1 ± 0.3	5.5 ± 1.0

ΔE = Color difference, ΔL* = Variation in luminosity, Δa* = Variation between red color and green, and Δb* = Variation between yellow and blue

UV, WI-70, and OI-70 samples have the highest color difference (ΔE) of all conditions. As the temperature of OI samples rises, ΔE rises as well. The WI-RT and WI-50 samples, on the other hand, had minor changes and were statistically equal.

The results of the colorimetric tests were interpreted for each condition in **Table 7**. Changes in UV, WI-70, OI-50, and OI-70 samples could be visible to anyone, which makes sense when looking at Figure 7 and seeing how those groups stand out more. Tensile samples were generally lighter and redder than AR samples.

Table 7. Interpretation of the values of ΔE, ΔL*, Δa*, and Δb* of the tensile samples.

Condition	ΔE	ΔL*	Δa*	Δb*
AR	-	-	-	-
UV	Visible to anyone	Lighter	Greener	Yellower

WI-RT	Visible to trained operators	Lighter	Redder	Bluer
WI-50	Visible to trained operators	Darker	Greener	No change
WI-70	Visible to anyone	Darker	Redder	Yellower
OI-RT	Visible to trained operators	Lighter	Redder	Bluer
OI-50	Visible to anyone	Lighter	Redder	Bluer
OI-70	Visible to anyone	Lighter	Redder	Yellower

3.2. OPS samples

Mechanical tests were performed on samples of the ortho-planar spring specimen. **Table 8** shows the mean values of mechanical properties for each condition, such as spring constant, force at 20% deflection of flexible member length (FML), and Young's modulus of flexible member (FM). **Figure 11** shows the mechanical test results of one OPS sample from each condition. Each mechanism was tested five times, with a displacement of 20% FML (10.30mm) applied in each test. The plots of the tensile tests of all samples can be found in the Supporting Information in **Figure S9**, **S10**, **S11**, **S12**, **S13**, **S14**, **S15** and **S16**.

Table 8. Mechanical properties of the OPS samples.

Condition	Spring constant [N.m]	Force at 20% FML [N]	Young's modulus of FM [MPa]
AR	1439.9 ± 115.3	23.4 ± 3.3	1647.4 ± 72.6
UV	1335.7 ± 36.2	21.4 ± 1.0	1617.1 ± 279.8
WI-RT	1562.5 ± 63.9	27.5 ± 1.9	1881.8 ± 273.6

WI-50	1348.1 ± 105.1	18.9 ± 5.3	1417.3 ± 345.1
WI-70	1507.8 ± 75.4	27.0 ± 4.7	1710.6 ± 295.7
OI-RT	1408.1 ± 99.2	25.4 ± 7.8	1706.4 ± 283.5
OI-50	1529.3 ± 141.6	26.2 ± 3.1	1572.5 ± 347.1
OI-70	1513.2 ± 180.2	26.0 ± 7.1	1556.2 ± 195.8

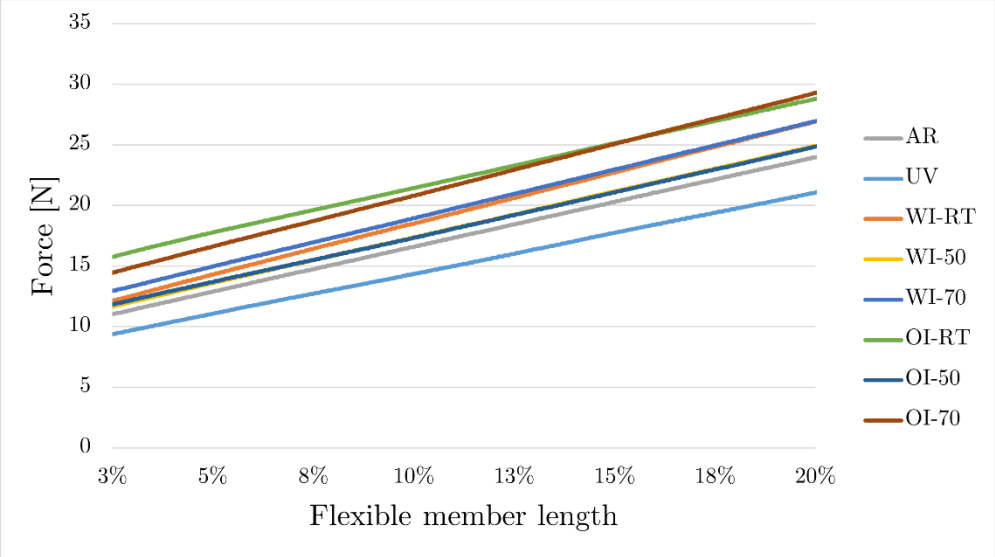

Figure 11. Mechanical tests of one OPS sample of each condition.

The mechanical properties of OPS samples were corrected, and the p-value for each condition of the Student's t-test for all properties is listed in **Table 9**. In **Figure 12**, it is shown the variations in the corrected mechanical properties. Unless otherwise stated, all discussions of results will now be based on the corrected values.

Table 9. The p-value of the Student's t-test of the corrected mechanical properties of the OPS samples.

Condition	Spring constant	Force at 20% FML	Young's modulus

			of FM
AR	-	-	-
UV	0.9167	0.8350	0.6038
WI-RT	0.9394	0.9489	0.9086
WI-50	0.6717	0.8211	0.7792
WI-70	0.7013	0.8096	0.5806
OI-RT	0.5090	0.6843	0.6945
OI-50	0.8603	0.8770	0.5513
OI-70	0.8863	0.8002	0.5693

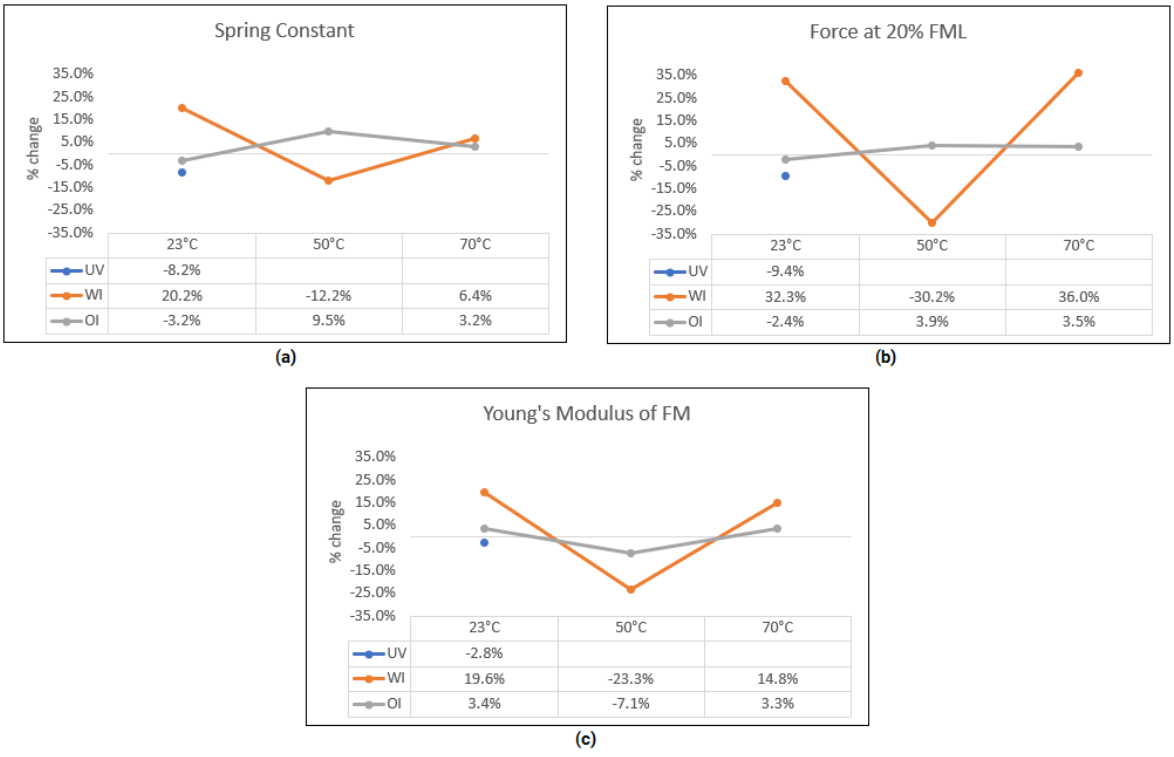

Figure 12. Variations of the mechanical properties of the OPS samples as a function of temperature.

The mechanical behavior of OPS samples differed from the expected linear results, with two distinct slope regions being present instead of one. The displacement axis (x-axis) of **Figure 11** begins in 3% FML to show only the linear behavior of the mechanisms. One possible

cause for this issue may be related to the universal testing machine and ABS parts of the setup, because the testing equipment and ABS parts are not considered rigid and suffer displacements during the test. Empirically, it was found that this phenomenon is more common in the range of forces from 0 N to 15 N. As the tests of the mechanisms stayed just above this range, the testing setup may have had an impact on the results and the expected linear behavior since the start was not present.

The spring constant was calculated using the slope of the straight line between 3% and 20% FML, which is when the spring begins to behave linearly as expected. The results in **Table 9** for the spring constant and force at 20% FML would be more relevant if the mechanical tests did not reveal the mentioned issue and sample geometric variation was not significant.

An alternative to check the effect of aging in OPS samples is to check how the Young's modulus of the flexible members has changed. This can be accomplished by using

$$\mathrm{E} = \frac{L^3}{18I\delta_p}\mathrm{F} \tag{2}$$

where E is Young's modulus, L is the length of the flexible member, F is the force at 20% FML, and δ_p the displacement at 20% FML [8]. I is the moment of inertia, which takes the average width of all FMs and the height of the mechanism into account. This equation was used and the data was presented in **Table 8**.

According to the p-values in **Table 9**, only the spring constant of UV samples and the properties of WI-RT samples are statistically different from the AR samples. Therefore, it is not possible to say that aging had a significant impact on the mechanical behavior of the mechanisms. This is an interesting result, indicating that ortho-planar springs' elastic properties remain somewhat intact after 6 months of harsh aging conditions such as water and oil immersion, as well as UV radiation.

The samples' weights were measured before and after the aging processes, and the results are listed in **Table 10**. The WI and OI samples absorbed the same amount of liquid. The UV

samples had a modest weight variation due to moisture absorption inside the UV dark chamber. Because the global average infill of OPS samples was 91.3%, while the infill of tensile samples was 74.6%, the difference in weight variations of both types of specimens is due to the fact that samples with a higher infill percentage will present fewer voids and paths for the liquid to enter and interact with.

Table 10. Weight of the OPS samples before and after the aging processes.

Condition	Weight [g]	Weight after [g]	Variation
AR	24.6 ± 0.7	-	-
UV	24.3 ± 0.4	24.4 ± 0.4	+0.5%
WI-RT	24.8 ± 0.2	25.6 ± 0.3	+3.3%
WI-50	23.4 ± 1.3	24.5 ± 1.1	+4.8%
WI-70	25.5 ± 0.4	26.7 ± 0.8	+4.8%
OI-RT	24.4 ± 1.2	25.3 ± 1.2	+3.5%
OI-50	25.3 ± 0.2	26.4 ± 0.1	+4.3%
OI-70	24.4 ± 1.4	25.5 ± 1.4	+4.6%

The most noticeable color change was seen in UV, WI-70, and OI-70 samples. OI-70 samples were lighter than WI-70 samples despite absorbing the most oil, indicating chemical degradation of WI-70 samples. The color of WI-70 and OI-70 samples shifted from white to a brown scale, while UV samples tended to a light-yellow tone. **Figure 13** shows the samples from all of the conditions.

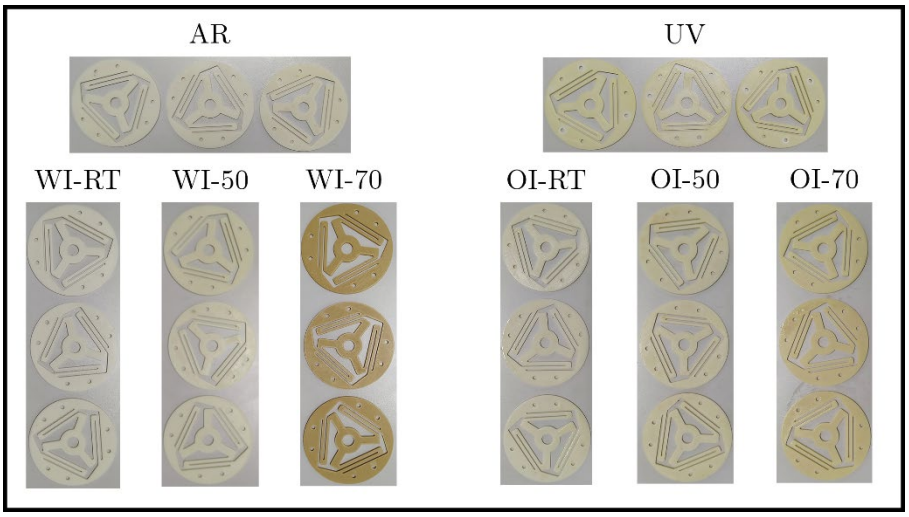

Figure 13. OPS samples after aging and mechanical tests.

Colorimetric tests were performed on OPS samples, and the values of ΔE, ΔL*, Δa*, and Δb* for each condition are shown in **Table 11**.

Table 11. Values of ΔE, ΔL*, Δa*, and Δb* of the OPS samples.

Condition	ΔE	ΔL*	Δa*	Δb*
AR	-	-	-	-
UV	10.1 ± 0.9	1.3 ± 2.0	-0.7 ± 0.1	9.8 ± 0.8
WI-RT	6.8 ± 0.5	6.7 ± 0.6	-0.1 ± 0.1	-0.7 ± 1.2
WI-50	6.8 ± 0.5	6.5 ± 0.5	-0.5 ± 0.1	2.1 ± 0.2
WI-70	18.1 ± 0.7	-4.7 ± 2.7	5.0 ± 0.2	16.6 ± 0.2
OI-RT	2.7 ± 0.6	2.5 ± 0.5	-0.4 ± 0.2	-0.7 ± 0.6
OI-50	3.0 ± 1.4	0.7 ± 2.4	-0.5 ± 0.1	2.2 ± 1.2
OI-70	7.8 ± 1.2	-1.2 ± 3.3	-0.3 ± 0.2	7.2 ± 0.8

ΔE = Color difference, ΔL* = Variation in luminosity, Δa* = Variation between red color and green, and Δb* = Variation between yellow and blue

UV, WI-70, and OI-70 samples have the highest color difference (ΔE) of all conditions. Despite being significant, the changes in room temperature and 50°C in the immersed samples did not appear to be caused by temperature but instead appeared to be caused by the liquid with which they were in contact. Color differences in both liquids were evident in samples immersed and at 70°C, indicating the impact of temperature.

The increase in color difference with the increase in temperature was already seen in other works. Pereira et al. [27] investigated how temperature, aging time, and oil type affected the color difference in aged samples. They noticed that when comparing 50°C and 70°C aged samples, the increase in ΔE was more significant, which is also seen in this study. When the temperature was raised from 70°C to 90°C, the variation was minimal, indicating that the samples had reached a saturation level. The aging temperature was the most important variable. The aging time is important as well, but not to the same extent as the temperature. The color was also affected by the type of oil used, but the variation profile was consistent across all oil types.

The results of the colorimetric tests were interpreted for each condition in **Table 12**. Changes in OI-RT and OI-50 samples could be visible to trained operators and the rest were visible to anyone. OPS were generally darker, greener, and yellower than AR samples.

Table 12. Interpretation of the values of ΔE, ΔL*, Δa*, and Δb* of the OPS samples.

Condition	ΔE	ΔL*	Δa*	Δb*
AR	-	-	-	-
UV	Visible to anyone	Darker	Greener	Yellower
WI-RT	Visible to anyone	Darker	Greener	Bluer
WI-50	Visible to anyone	Darker	Greener	Yellower
WI-70	Visible to anyone	Lighter	Redder	Yellower

OI-RT	Visible to trained operators	Darker	Greener	Bluer
OI-50	Visible to anyone	Darker	Greener	Yellower
OI-70	Visible to anyone	Lighter	Greener	Yellower

ΔE = Color difference, ΔL* = Variation in luminosity, Δa* = Variation between red color and green, and Δb* = Variation between yellow and blue

5. Conclusion

To determine how aging affects compliant mechanisms' mechanical behavior and elastic capabilities, 48 samples (6 non-aged and 42 aged) were mechanically tested. The mechanisms were expected to change because polymers degrade and lose mechanical properties under these conditions. Tensile sample infill averaged 74.6%, below the expected 100%. However, mechanical properties of each condition were compared. Here are the main remarks obtained from this work:

- Apart from a possible chemical degradation indicated by a change in material color, it was not possible to confirm that aging was indeed responsible for the reported mechanical property decreases or increases.
- The Infill percentage (91.3%) and geometric dimensions of OPS samples were close to expected. The standard deviations of the properties of aged samples show that aging did affect the samples, but not enough to notice the effect of aging on OPS samples' mechanical properties.
- Tensile samples' Young's modulus decreased in WI-70 (-17.9%), OI-RT (-16.2%), and OI-70 (-15.8%). Moisture absorption in the UV dark chamber caused UV samples to have a decrease of 14.5%. Elongation at break of UV and OI samples was also affected. Microcracks in UV-exposed samples decreased this property, while plasticization in oil-immersed samples increased it.

- Colorimetric tests showed significant color shifts. UV, WI-70, and OI-70 suffered most. Previous research showed that UV radiation yellows polymers, so UV samples were expected to change. WI and OI samples differed more with temperature, especially from 50°C to 70°C. Pereira et al. [32] showed that sample colors reach saturation level at temperatures near 90°C.
- Young's modulus and elongation at break had significant variations in tensile samples, unlike OPS samples. UV exposure, water immersion, and oil immersion did not significantly affect OPS samples mechanical properties.

Popescu et al. [31] tested 3D printed ABS for natural aging (normal daylight changes) and multiple sterilizations to simulate hospital conditions for medical instruments. Tensile and flexural tests showed no significant difference between standard specimens after aging to unaged samples. The authors go on to say that 3D-printed ABS can make medical instruments. When we connect the results of Popescu et al. [31] with the ones from this study, it can be said that compliant mechanism made with ABS may have promising use in applications that are subjected to aging environments.

The ortho-planar spring of this work, considering the test conditions used, maintained its original mechanical properties and elastic capabilities after six months of aging. Although tests using different materials, environments, and exposure times would be needed to verify use in a specific situation, the results of this study suggest that compliant mechanisms show promise for implementation in applications where aging is a concern, and their lifetime is expected to be within the bounds of this aging study.

Supporting Information

Supporting Information is available from the author.

Acknowledgements

The authors acknowledge the financial support of CAPES and CNPq in the development of this work.

Received: ((will be filled in by the editorial staff))
Revised: ((will be filled in by the editorial staff))
Published online: ((will be filled in by the editorial staff))

References

[1] Howell, L. L., *Compliant Mechanisms*, John Wiley & Sons, **2001**.

[2] George B, L., Bharanidaran, R., *Aust. J. Mech. Eng.* **2020**, 4846.

[3] Rubbert, L., Renaud, P., Caro, S., Gangloff, *J. Mech. Ind.* **2014**, *15*, 147.

[4] Mareta, S., Halim, D., Popov, A. A., *2015 IEEE Int. Conf. Mechatronics Autom. ICMA 2015* **2015**, 1875.

[5] Prakashah, H. N., Zhou, H., *J. Mech. Robot.* **2016**, *8*, 1.

[6] Hu, R., Venkiteswaran, V., Su, H., *J. Mech. Mach. Sci.* **2019**, *66*, 33.

[7] Miao, Y., Zheng, J., *Comput. Electron. Agric.* **2020**, *170*, 105232.

[8] Parise, J. J., Howell, L. L., Magleby, S. P., *Mech. Mach. Theory* **2001**, *36*, 1281.

[9] Wang, W., Wu, X., Ding, C., Huang, X., Ye, N., Yu, Q., Mai, K., *J. Appl. Polym. Sci.* **2021**, *138*, 50948.

[10] Moghtadernejad, S., Barjasteh, E., Johnson, Z., Stolpe, T., Banuelos, J., *J. Appl. Polym. Sci.* **2021**, *138*, 50211.

[11] Jubinville, D., Abdelwahab, M., Mohanty, A. K., Misra, M., *J. Appl. Polym. Sci.* **2020**, *137*, 48618.

[12] Santos, L. F. L., *Bachelor's Thesis*, Rio de Janeiro State University, **2019**.

[13] Becerra, A. F. C., D'Almeida, J. R. M., *Polym. Polym. Compos.* **2017**, *25*, 327.

[14] Vichi, A., Ferrari, M., Davidson, C. L., *Dent. Mater.* **2004**, *20*, 530.

[15] Hedir, A., Moudoud, M., Lamrous, O., Rondot, S., Jbara, O., Dony, P., *J. Appl. Polym. Sci.* **2020**, *137*, 48575.

[16] Kumar, BG., Singh, RP., Nakamura, T., *J. Compos. Mater.* **2002**, *36*, 2713.

[17] Capiel, G., Uicich, J., Fasce, D., Montemartini, P. E., *Polym. Degrad. Stab.* **2018**, *153*, 165.

[18] De Parscau Du Plessix, B., Jacquemin, F., Lefébure, P., Le Corre, S., *J. Compos. Mater.* **2016**, *50*, 2495.

[19] Robert, M., Wang, P., Cousin, P., Benmokrane, B., *J. Compos. Constr.* **2010**, *14*, 361.

[20] Shi, C., Tang, Z., Wang, S., *IEEE Trans. Med. Robot. Bionics* **2021**, *3*, 362.

[21] Wu, K., Zheng, G., Hao, G., *Mech. Mach. Theory* **2021**, *162*, 104343.

[22] Liu, Y., Mo, S., Shang, S., Wang, H., Wang, P., Yang, K., *Energies* **2020**, *13*, 5919.

[23] ASTM D638-14, *ASTM International*, West Conshohocken, PA, **2014**.

[24] Amaral, D. L., *Bachelor's Thesis*, Rio de Janeiro State University, **2020**.

[25] Wang, S., Ma, Y., Deng, Z., Zhang, S., Cai, *J. Polym. Test.* **2020**, *86*, 106483.

[26] Kajorncheappunngam, S., Gupta, R. K., GangaRao, H. V. S. *J. Compos. Constr.* **2002**, *6*, 61.

[27] Pereira, A. A. C., *Master's Thesis*, Pontifical Catholic University of Rio de Janeiro, **2019**.

[28] Fiorio, R., Díez, S. V., Sánchez, A., D'hooge, D. R., Cardon, L. *Materials (Basel)*. **2020**, *13*.

[29] Desloir, M., Benoit, C., Bendaoud, A., Alcouffe, P., Carrot, C. *J. Appl. Polym. Sci.* **2019**, *136*, 1.

[30] Kakanuru, P., Pochiraju, K. *Addit. Manuf.* **2020**, *36*, 101529.

[31] Popescu, D., Baciu, F., Vlasceanu, D., Cotrut, C. M., and Marinescu, R. *Mech. Mater.*, **2020**, 148, 103423.

[32] Pereira, A. A. C., Becerra, A. F. C., D'Almeida, J. R. M. *Brazilian Conference of Engineering and Science of Materials*, Foz do Iguaçu, **2018**, pp 8007.

Ortho-planar spring compliant mechanism samples were analyzed in this work to understand how aging conditions such as ultraviolet radiation, water immersion and oil immersion would affect their mechanical properties and elastic capabilities. Even after six months of harsh aging conditions, no significant changes were detected in the mechanisms, which is an interesting result.

L. F. L. Santos*, J. R. M. d'Almeida and L. L. Howell

Changes in the mechanical performance of an ortho-planar spring after aging tests

New references added above (check to make sure that these aren't duplicates of any already in the paper):

Rasmussen, N. O., Todd, R. H., Howell, L. L., & Magleby, S. P. (2006, January). Investigation of compliant ortho-planar springs for rotational applications. In *International Design Engineering Technical Conferences and Computers and Information in Engineering Conference* (Vol. 42568, pp. 159-171).

"Continuously Variable Transmission or Clutch with Ortho-Planar Compliant Mechanism," Whiting, M.J., Howell, L.L., Todd, R.H., Magleby, S.P., Anderson, M.C., and Rasmussen, N.O., U.S. Patent No. 7,338,398, issued March 4, 2008

Qi, P., Qiu, C., Liu, H., Dai, J. S., Seneviratne, L. D., & Althoefer, K. (2015). A novel continuum manipulator design using serially connected double-layer planar springs. IEEE/ASME Transactions on Mechatronics, 21(3), 1281-1292.

Dhote, S., Li, H., & Yang, Z. (2019). Multi-frequency responses of compliant orthoplanar spring designs for widening the bandwidth of piezoelectric energy harvesters. International Journal of Mechanical Sciences, 157, 684-691.

Shi, C., Tang, Z., & Wang, S. (2021). Design and experimental validation of a fiber Bragg grating-enabled force sensor with an ortho-planar spring-based flexure for surgical needle insertion. IEEE Transactions on Medical Robotics and Bionics, 3(2), 362-371.

Nguyen, N. T., Truong, T. Q., Wong, K. K., Ho, S. S., & Low, C. L. N. (2003). Micro check valves for integration into polymeric microfluidic devices. Journal of Micromechanics and Microengineering, 14(1), 69.

Konstantinova, J., Stilli, A., & Althoefer, K. (2017). Fingertip fiber optical tactile array with two-level spring structure. Sensors, 17(10), 2337.
Ataollahi, A., Fallah, A. S., Seneviratne, L. D., Dasgupta, P., & Althoefer, K. (2012). Novel force sensing approach employing prismatic-tip optical fiber inside an orthoplanar spring structure. IEEE/ASME Transactions on Mechatronics, 19(1), 121-130.

Teichert, G. H., Burnett, S., & Jensen, B. D. (2013). A microneedle array able to inject tens of thousands of cells simultaneously. Journal of Micromechanics and Microengineering, 23(9), 095003.

Lyu, Z., & Xu, Q. (2022, July). Design of a Compliant Vertical Micropositioning Stage Inspired by Lamina Emergent Mechanism. In 2022 International Conference on Manipulation, Automation and Robotics at Small Scales (MARSS) (pp. 1-6). IEEE.